SAND2013-4517C

A SYSTEMATIC STUDY OF CURRENT FLOW AND IMPEDANCE BEHAVIOR IN THE Z MACHINE DOUBLE POST-HOLE CONVOLUTE *

M. R. Gomez ξ, M. E. Cuneo, J.-P. Davis, R. W. Lemke,
R. D. McBride, R. B. Campbell, W. A. Stygar
Sandia National Laboratories, PO Box 5800, Mail Stop 1193
Albuquerque, NM, USA

D. V. Rose, D. R. Welch, E. A. Madrid
Voss Scientific, LLC, 418 Washington Dr. SE
Albuquerque, NM, USA

Abstract

Sandia's Z-Facility is used to conduct high energy density science experiments. Large pulsed power drivers, such as Z, are designed to deliver a large current with a short risetime to a magnetically-driven load. This often requires the use of multiple self-magnetically insulated transmission lines (MITL) in parallel to reduce inductance. The MITL currents must be recombined into a single anode-cathode gap at the load, often through a post-hole convolute. Efficient post-hole convolute operation is necessary to maximize the current delivered to the load.

The Z machine utilizes four parallel MITLs and a double post-hole convolute. The current at several radial locations in the MITLs is inferred from B-dot monitor measurements. The MITL current downstream of the convolute can be several Mega-amperes less than the sum of the currents flowing in the MITLs upstream of the convolute. A systematic study of the convolute shunt current and convolute impedance for several types of Z experiments has been conducted. Convolute behavior is highly dependent on convolute voltage, which is a strong function of load type. Variations for nominally identical experiments are measurable, but small by comparison.

I. INTRODUCTION

Sandia National Laboratories' Z-Facility [1, 2] is the world's largest pulsed power facility. High energy density science experiments conducted at the Z-Facility range from dynamic material strength measurements [3] to high photon energy, intense x-ray source studies [4] to inertial confinement fusion experiments [5]. The Z-machine is a Marx-bank-based pulsed power driver that utilizes pulse-charged intermediate storage capacitors and switches for pulse compression [2]. Z can deliver up to 27 MA with a sub-100 ns risetime to the vacuum insulating stack [1]. Energy is coupled from the insulating stack to the load via four parallel magnetically insulated transmission lines (MITL) as shown in Fig. 1.

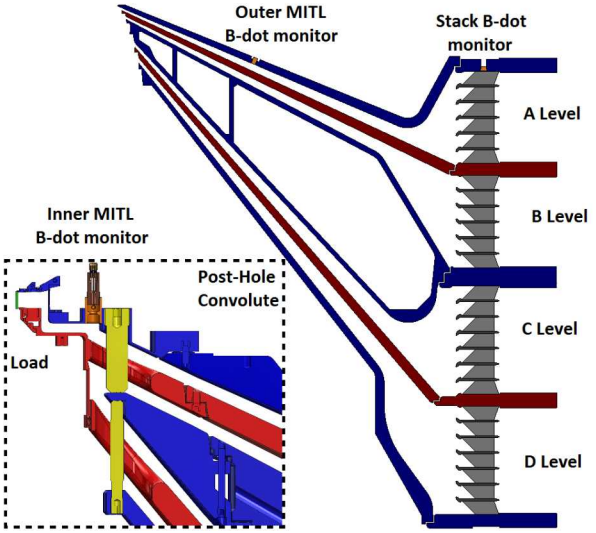

Figure 1. An R-Z section of a CAD model of the Z vacuum section. The inset in the lower left corner shows the double post-hole convolute. Anodes are depicted in blue, cathodes in red, and the convolute posts are yellow. B-dot monitor locations are also shown.

A double post-hole convolute [6, 7] is used to combine the current from the four MITLs at the load. Current is inferred from B-dot monitor signals at several radial locations in the MITLs; monitors are located at the stack (Stack current), the midpoint of the MITLs (MITL

* Sandia National Laboratories is a multi-program laboratory managed and operated by Sandia Corporation, a wholly owned subsidiary of Lockheed Martin Corporation, for the U.S. Department of Energy's National Nuclear Security Administration under contract DE-AC04-94AL85000.
ξ email: mrgomez@sandia.gov

current), and downstream of the convolute (Inner MITL current) [8]. In most experiments, the inner MITL current is less than expected based on the stack current, which indicates a loss in the vacuum section [9].

The MITL current typically matches the stack current to within the uncertainty in the measurement (see Fig. 2). Due to displacement current effects, a lossless propagation of the stack current through the convolute (Translated Stack current) must be applied prior to comparing with the inner MITL current [10]. There is a clear difference between the translated stack current and the inner MITL current for nearly all experiments on Z (see Fig. 2 for an example). The "apparent loss" current [11] is referred to as the Convolute Shunt current, which is defined as the difference between the translated stack current and the inner MITL current.

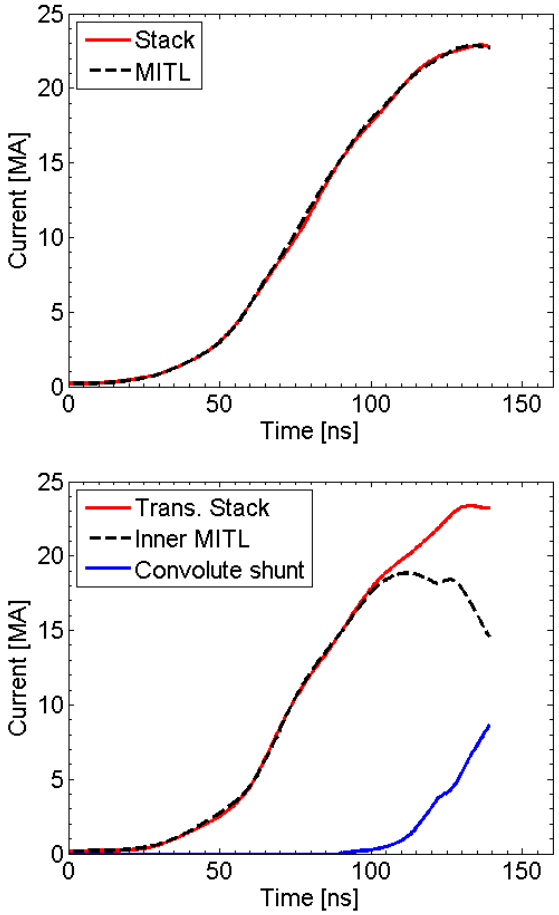

Figure 2. Plots of the current traces from z2082. The upper plot shows the stack and MITL currents which match to within the precision of the measurement. The lower plot shows a lossless propagation of the stack current to the load (trans. stack), the inner MITL current, and the difference between them (convolute shunt current).

It is important to note that the convolute shunt current is not the same as the current lost due to convolute inefficiency (Loss current) [11]. The loss current is defined as the difference between the inner MITL current without convolute loss and the inner MITL current with convolute loss. BERTHA [12] was used to simulate the effect of convolute loss on the inner MITL current for z2333. In the simulation, convolute loss was turned off to determine the inner MITL current without convolute loss (No Loss current). The no loss current falls in between the translated stack current and the inner MITL current with convolute loss (see Fig. 3). The convolute shunt current and the loss current for this example are also shown in Fig. 3.

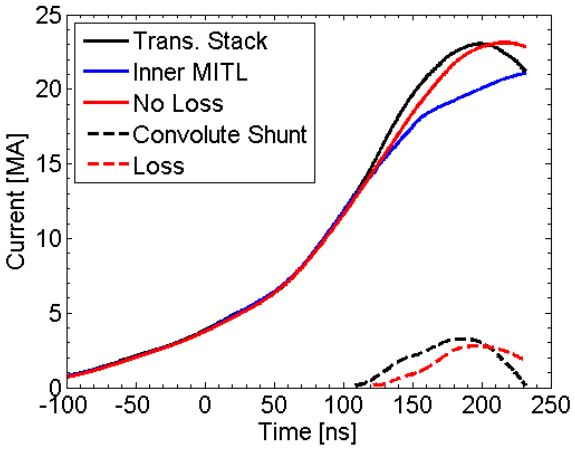

Figure 3. A plot of the experimental stack current losslessly propagated through the convolute (trans. stack), experimental inner MITL current, and the simulated no loss current traces generated in BERTHA for z2333. The convolute shunt current (trans. stack – inner MITL) and the loss current (no loss – inner MITL) are also plotted. The convolute shunt current exceeds the loss current throughout most of the current pulse.

The convolute voltage was calculated using voltage measured at the stack and the transmission line model described in [10]. The convolute impedance is defined as the convolute voltage divided by the shunt current.

In this paper the convolute voltage, the convolute shunt current, and the convolute impedance are calculated for many experiments. Nominally identical experiments are compared to establish reproducibility of convolute behavior. Various experiment types are compared to establish trends in losses with load type and machine configuration.

II. DISCUSSION

A wide variety of load types and current pulse shapes are used on Z. The majority of Z experiments experience some loss attributed to the convolute. Some experiments experience acceptable losses on the order of 1 MA, while others are plagued by multi-MA losses.

Ignoring losses, the current delivered to the load is still highly dependent on the load type and driving voltage

pulse shape. The driving voltage and current are related by

$$V(t) = L(t)*dI/dt + dL/dt*I(t) \quad (1)$$

where V is the driving voltage, L is the inductance of the system, and I is the current through the system. Experiments with large L or rapid increases in L have lower peak current. The dynamic hohlraum [13] is an example of a high peak current experiment, and the radiation effects experiments [4] typically have low peak current as shown in Fig. 4. These two experiments are interesting to study because they are examples of good and poor convolute performance. Additionally, there is a large data set of nominally identical experiments (20+) for each type of experiment.

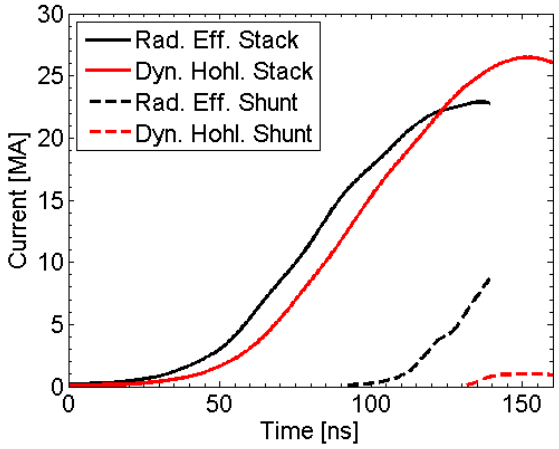

Figure 4. A plot of the stack current and convolute shunt current for a radiation effects experiment (z2082) and a dynamic hohlraum experiment (z2410). The radiation effects stack current rises sooner because the initial inductance of the system is lower. The peak stack current is lower for the radiation effects experiment because the inductance increases much faster. The convolute shunt current for the radiation effects experiment is much larger and occurs much sooner.

A. Convolute Behavior Variations for Nominally Identical Experiments

Z experiments with nominally identical loads have variations in peak load current and x-ray power. It follows that the convolute behavior may also vary for nominally identical experiments. In order to establish a correlation between a change in convolute behavior and load type, the change must be outside the variations in convolute behavior for nominally identical experiments.

A total of 24 radiation effects experiments between z2077 and z2504 were studied. These experiments all used approximately 8.5 micron diameter stainless steel wire in 20 mm tall 70 mm/35 mm diameter nested arrays. Wire number varied between 108/54 and 112/56 to maintain the same imploding mass. The convolute voltage and convolute shunt current for each experiment is plotted in Fig. 5. Each trace has been time shifted so the convolute voltage at 60 ns is 1 MV. There is a noticeable spread in the shape of the convolute voltage and the start time of the convolute shunt current. The time from 1 MV convolute voltage to 0.5 MA convolute shunt current for these experiments is 50 +/- 6 ns.

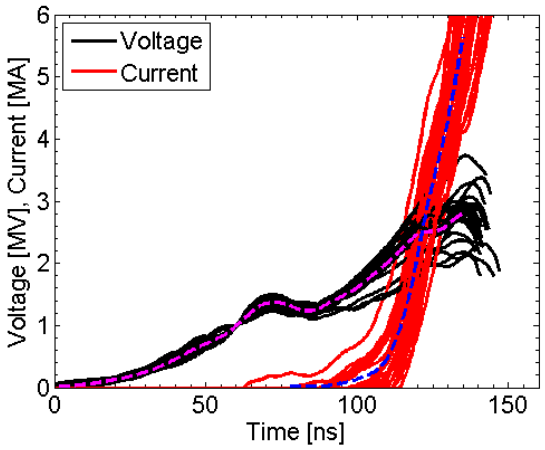

Figure 5. A plot of the convolute voltage and convolute shunt current for 24 nominally identical radiation effects experiments. The average voltage is shown in dashed magenta, and the average current is shown in dashed blue.

Typically small variations in the convolute shunt current behavior are linked to variations in the convolute voltage. Experiments with a delayed rise in the second portion of the voltage pulse also have a delayed convolute shunt current (see Fig. 6). Variations in the convolute voltage could arise from small variations in the Z voltage drive and/or variation in load performance.

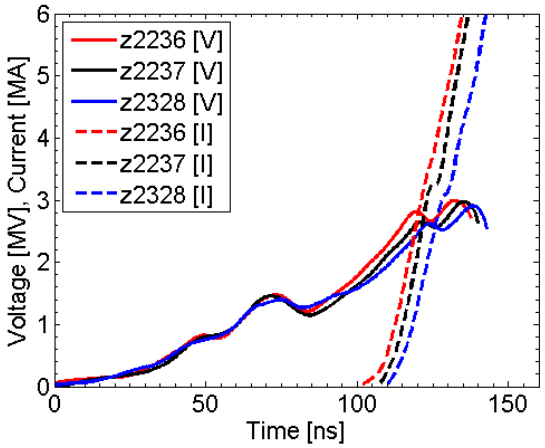

Figure 6. A plot of the convolute voltage and convolute shunt current for three nominally identical radiation effects experiments. The start time of the convolute shunt current is later for experiments with lower convolute voltage.

There are cases which deviate from this trend as shown in Fig. 7. Despite nearly identical convolute voltages, compared to z2237, z2168 has a significant foot on the

convolute shunt current. This could be the result of a difference in hardware machining or processing, or variations in the contamination of the hardware. The convolute shunt current behavior for both experiments follows the same late time trend, which indicates that the cause of the foot is not the dominant loss mechanism.

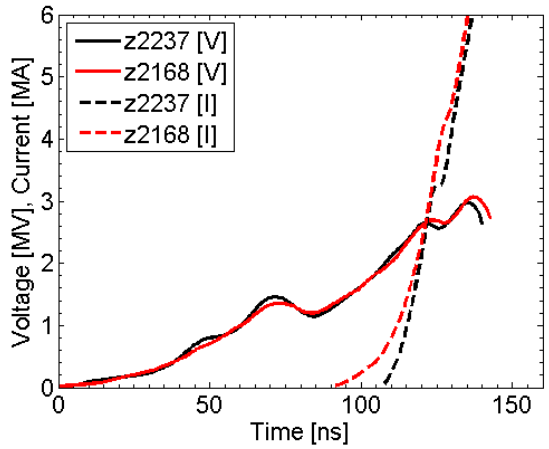

Figure 7. A plot of the convolute voltage and convolute shunt current for two nominally identical radiation effects experiments. Z2237 displays typical convolute shunt current behavior, and z2168 has a foot on the convolute shunt current despite nearly identical convolute voltage to z2237. Both experiments follow the same late time trend.

The analysis listed above was repeated for a set of 37 nominally identical dynamic hohlraum experiments. These experiments all used approximately 11.2 micron diameter tungsten wires in a 12 mm tall 40 mm/20 mm diameter, 240/120 wire, nested array with a 6 mm diameter, 14.5 mg/cc foam on axis. The convolute voltage and convolute shunt current for each experiement is plotted in Fig. 8. The time from 1 MV convolute voltage to 0.5 MA convolute shunt current for these experiments is 74 +/- 5 ns.

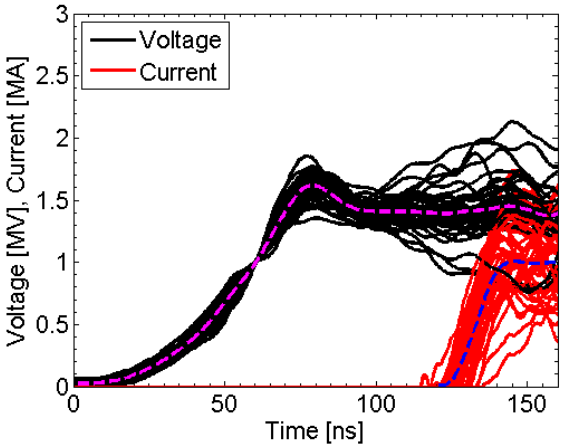

Figure 8. A plot of the convolute voltage and convolute shunt current for 37 nominally identical dynamic hohlraum experiments. Average voltage shown in dashed magenta, and average current shown in dashed blue.

The difference in convolute behavior for each set of nominally identical experiments was small compared to the difference between the two sets. This indicates that differences observed in convolute behavior for the different experiment types are not due to random fluctuations within a data set, and are attributable to the change in the experiment configuration.

B. Convolute Behavior for Different Load Types

The convolute behavior was compared for three types of wire array loads. The loads include the radiation effects array and the dynamic hohlraum array described above and a soft x-ray producing tungsten array with approximately 5.5 micron diameter tungsten wires in a 20 mm tall, 65 mm/32.5 mm diameter, 192/96 wire, nested array. The convolute voltage and convolute shunt current are plotted in Fig. 9 for these cases. The start time of the convolute shunt current is earlier and the amplitude of the convolute shunt current is greater for larger convolute voltage. This is consistent with speculation that high voltage in the convolute causes plasma formation and current is lost via the plasma [14, 15].

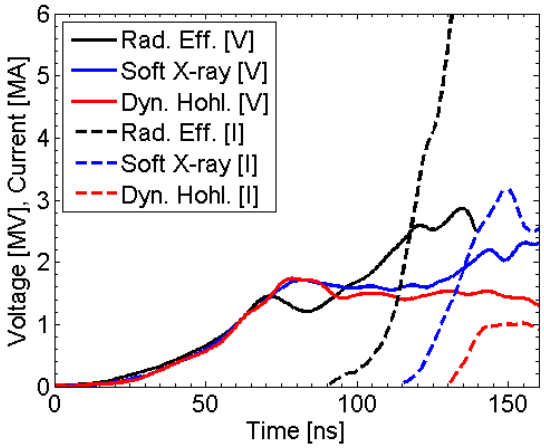

Figure 9. A plot of the convolute voltage and convolute shunt current for a radiation effects experiment (z2082), a soft x-ray generation experiment (z2305), and a dynamic hohlraum experiment (z2410). The convolute shunt current occurs later and peaks at a lower value for experiments with lower convolute voltage.

The analysis described above was expanded to the cylindrical liner loads central to the MagLIF concept [16]. Three types of cylindrical liner experiments were examined, the baseline MagLIF design, a long pulse version, and a low charge voltage version. The convolute voltage and convolute shunt currents for these experiments are shown in Fig. 10.

This plot shows a number of effects that were not apparent from the wire array data. Perhaps most importantly, the low charge voltage data show that there appears to be a threshold convolute voltage below which there are no convolute losses. Additionally, the long pulse data show that sub-1 MV voltages can exist for long

periods without negatively impacting the convolute performance. Finally, the standard data show that once the convolute loss mechanism is enabled, it will persist despite a drop in voltage.

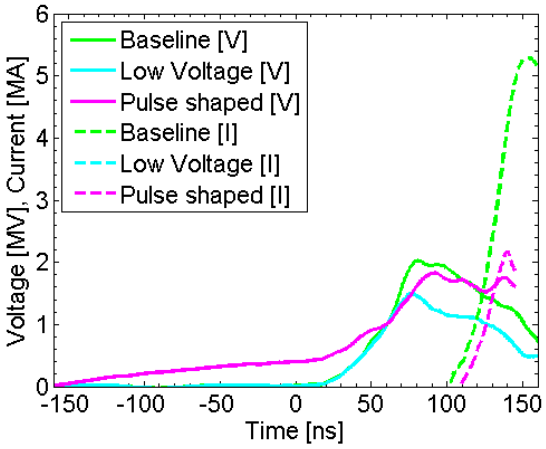

Figure 10. A plot of the convolute voltage and convolute shunt current for three cylindrical liner experiments: the baseline liner experiment (z2390), a low voltage, high aspect ratio experiment (z2416), and a low aspect ratio pulse shaped experiment (z2208). The convolute shunt current for the low voltage experiment was less than the uncertainty in the measurement.

Combining the cylindrical liner data with the wire array data gives a good picture of the overall convolute behavior (see Fig. 11). In all cases, higher convolute voltage leads to earlier and higher convolute shunt current.

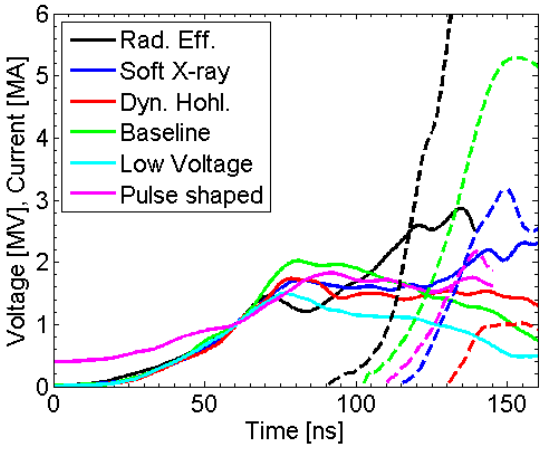

Figure 11. A plot of the convolute voltage and convolute shunt current for three different wire array experiments and three different cylindrical liner experiments. The convolute shunt current occurs later and peaks at a lower value for experiments with lower convolute voltage.

The convolute impedance was calculated for each of the cases with nonzero convolute shunt current (see Fig. 12). In all cases, the convolute impedance rapidly drops to a relatively constant value. The time at which the impedance collapse occurs and the final impedance vary significantly from case to case. There is a clear trend of later collapse and higher final impedance for cases with lower convolute voltage. This indicates a non-linear dependence of the convolute shunt current on the convolute voltage.

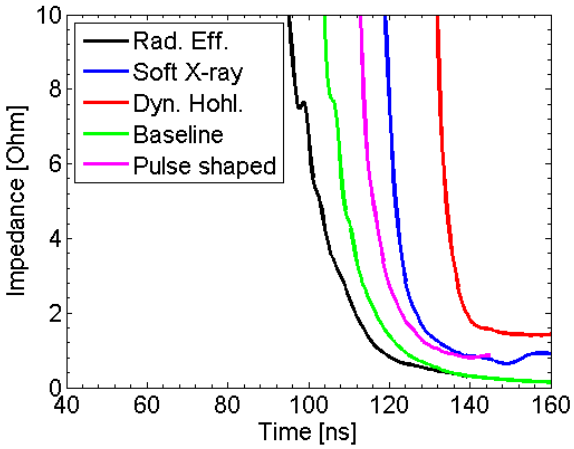

Figure 12. A plot of the convolute impedance for three different wire array experiments and two different cylindrical liner experiments. In all experiments the convolute experiences a rapid impedance collapse to a relatively constant value. The start time of the impedance collapse is later and the final impedance is higher for experiments with lower convolute voltage.

III. SUMMARY

The Z machine convolute behavior varies significantly depending on the load and machine configuration. Experiments that produce higher convolute voltage experience greater convolute shunt current. The convolute shunt current is only the "apparent loss" current, but the losses trend with the apparent loss. Not all of the apparent loss current would be recovered in a perfectly efficient convolute.

Variations in convolute behavior for nominally identical experiments are small compared to the change in behavior for different experiments. The small variations in convolute shunt current observed can typically be explained by small fluctuations in convolute voltage. Occasionally experiments deviate from the expected behavior at early times, which may be caused by contamination or production errors. This is not the dominant loss effect.

The impedance of the convolute rapidly drops to a relatively constant value for all experiments with measurable loss. The time to the collapse and the final impedance are higher for lower voltage experiments. This indicates that convolute performance is non-linearly related to convolute voltage.

IV. ACKNOWLEDGMENTS

We thank the entire Z team for successfully completing well over four hundred experiments in the last 3 years. J. K. Moore, M. E. Savage, and T. C. Wagoner were responsible for B-dot calibrations and raw signal processing. Data sets from experiments conducted by the following principle investigators were used in this analysis: D. J. Ampleford, J. E. Bailey, B. Jones, M. Jones, M. D. Knudsen, R. D. McBride, and D. B. Sinars.

V. REFERENCES

[1] M. E. Savage, K. R. LeChien, M. R. Lopez, B. S. Stoltzfus, W. A. Stygar, "Status of the Z Pulsed Power Driver" in Proceedings of the 18th International Pulsed Power Conference, 2011, pp. 983-990.

[2] D. V. Rose, D. R. Welch, E. A. Madrid, C. L. Miller, R. E. Clark, W. A. Stygar, M. E. Savage, G. A. Rochau, J. E. Bailey, T. J. Nash, M. E. Sceiford, K. W. Struve, P. A. Corcoran, B. A. Whitney, "Three-Dimensional electromagnetic Model of the Pulsed-Power Z-Pinch Accelerator," Physical Review Special Topics – Accelerators and Beams 13, 010402 (2010).

[3] J.-P. Davis, C. Deeney, M. D. Knudsen, R. W. Lemke, T. D. Pointon, and D. E. Bliss, "Magnetically driven isentropic compression to multimegabar pressures using shaped current pulses on the Z accelerator" Physics of Plasmas 12, 056310 (2005).

[4] B. Jones, C. A. Coverdale, C. Deeney, D. B. Sinars, E. M. Waisman, M. E. Cuneo, D. J. Ampleford, P. D. LePell, K. R. Cochrane, J. W. Thornhill, J. P. Aprizese, A. Dasgupta, K. G. Whitney, R. W. Clark, J. P. Chittenden, "Implosion dynamics and K-shell x-ray generation in large diameter stainless steel wire array Z pinches with various nesting configurations" Physics of Plasmas 15, 122703 (2008).

[5] R. D. McBride, S. A. Slutz, C. A. Jennings, D. B. Sinars, M. E. Cuneo, M. C. Herrmann, R. W. Lemke, M. R. Martin, R. A. Vesey, K. J. Peterson, A. B. Sefkow, C. Nakhleh, B. E. Blue, K. Killebrew, D. Schroen, T. J. Rogers, A. Laspe, M. R. Lopez, I. C. Smith, B. W. Atherton, M. Savage, W. A. Stygar, J. L. Porter, "Penetrating Radiography of Imploding and Stagnating Beryllium Liners on the Z Accelerator" Phys. Rev. Lett. 109, 135004 (2012).

[6] R. B. Spielman, P. Corcoran, J. Fockler, H. Kishi, P. W. Spence, "A Double Post-Hole Convolute Diode for Z-Pinch Experiments on Saturn" in Proceedings of the 7th International Pulsed Power Conference, 1989, pp. 445-448.

[7] T. D. Pointon, W. A. Stygar, R. B. Spielman, H. C. Ives, K. W. Struve, "Particle-In-Cell Simulations of Electron Flow in the Post-Hole Convolute of the Z Accelerator" Physics of Plasmas 8, pp. 4534-4544 (2001).

[8] T. C. Wagoner, W. A. Stygar, H. C. Ives, T. L. Gilliland, R. B. Spielman, M. F. Johnson, P. G. Reynolds, J. K. Moore, R. L. Mourning, D. L. Fehl, K. E. Androlewicz, J. E. Bailey, R. S. Broyles, T. A. Dinwoodie, G. L. Donovan, M. E. Dudley, K. D. Hahn, A. A. Kim, J. R. Lee, R. J. Leeper, G. T. Leifeste, J. A. Melville, J. A. Mills, L. P. Mix, W. B. S. Moore, B. P. Peyton, J. L. Porter, G. A. Rochau, G. E. Rochau, M. E. Savage, J. F. Seaman, J. D. Serrano, A. W. Sharpe, R. W. Shoup, J. S. Slopek, C. S. Speas, K. W. Struve, D. M. Van De Valde, R. M. Woodring, "Differential-Output B-dot and D-dot Monitors for Current and Voltage Measurements on a 20-MA, 3-MV Pulsed-Power Accelerator," Physical Review Special Topics - Accelerators and Beams 11, 100401 (2008).

[9] M. R. Gomez, M. E. Cuneo, R. D. McBride, G. A. Rochau, D. J. Ampleford, J. E. Bailey, A. D. Edens, B. Jones, M. Jones, M. R. Lopez, M. E. Savage, D. B. Sinars, W. A. Stygar, "Spectroscopic measurements in the post-hole convolute on Sandia's Z-machine (Invited)" in Proceedings of the 18th International Pulsed Power Conference, 2011, pp. 688-695.

[10] R. D. McBride, C. A. Jennings, R. A. Vesey, G. A. Rochau, M. E. Savage, W. A. Stygar, M. E. Cuneo, D. B. Sinars, M. Jones, K. R. LeChien, M. R. Lopez, J. K. Moore, K. W. Struve, T. C. Wagoner, E. M. Waisman, "Displacement Current Phenomena in the Magnetically Insulated Transmission Lines of the Refurbished Z Accelerator" Physical Review Special Topics – Accelerators and Beams 13, 120401 (2010).

[11] E. A. Madrid, D. V. Rose, D. R. Welch, R. E. Clark, W. A. Stygar, M. E. Cuneo, M. R. Gomez, T. P. Hughes, T. D. Pointon, D. B. Seidel, "Steady-state operation of a post-hole convolute driven by high power magnetically insulated transmission lines: Effects of electron emission, ion emission, and geometric-parameter variations" manuscript in preparation (2013).

[12] D. D. Hinshelwood, Naval Research Laboratory Memorandum Report No. 5185 (1983).

[13] J. P. Apruzese, R. W. Clark, J. Davis, T. W. L. Sanford, T. J. Nash, R. C. Mock, D. L. Peterson, "Diagnosing the properties of dynamic hohlraums with tracer spectroscopy (invited)" Review of Scientific Instruments 77, 10F303 (2006).

[14] C. A. Jennings, J. P. Chittenden, M. E. Cuneo, W. A. Stygar, D. J. Ampleford, E. M. Waisman, M. Jones, M. E. Savage, K. R. LeChien, T. C. Wagoner, "Circuit Model for Driving Three-Dimensional Resistive MHD Wire Array Z-Pinch Calculations" IEEE Transactions on Plasma Science 38, No. 4, pp. 529-539 (2010).

[15] D. V. Rose, D. R. Welch, T. P. Hughes, R. E. Clark, W. A. Stygar, "Plasma evolution and dynamics in high-power vacuum-transmission-line post-hole convolutes" Physical Review Special Topics – Accelerators and Beams 11, 060401 (2008).

[16] S. A. Slutz, M. C. Herrmann, R. A. Vesey, A. B. Sefkow, D. B. Sinars, D. C. Rovang, K. J. Peterson, and M. E. Cuneo, " Pulsed-power-driven cylindrical liner implosions of laser preheated fuel magnetized with an axial field" Physics of Plasmas 17, 056303 (2010).